NUMERICAL SIMULATIONS AND ANALYSES OF BEAM-INDUCED DAMAGE TO THE TEVATRON COLLIMATORS*

A.I. Drozhdin†, N.V. Mokhov, D.A. Still, FNAL, Batavia, IL 60510, USA
R.V. Samulyak, BNL, Upton, NY 11973, USA

Abstract

Numerical simulations are performed to analyze the Tevatron collimator damage happened in December 2003 that was induced by a failure in the CDF Roman Pot detector positioning during the collider run. Possible scenarios of this failure resulted in an excessive halo generation and superconducting magnet quench are studied via realistic simulations using the STRUCT and MARS14 codes. It is shown that the interaction of a misbehaved proton beam with the collimators result in a rapid local heating and a possible damage. A detailed consideration is given to the ablation process for the collimator material taking place in high vacuum. It is shown that ablation of tungsten (primary collimator) and stainless steel (secondary collimator) jaws results in creation of a groove in the jaw surface as was observed after the December's accident.

INTRODUCTION

There are 24 cryogenic refrigerator houses for the Fermilab Tevatron ring. One house cryogenically keeps about 40 magnets at superconductng temperatures. On December 5, 2003, the Tevatron suffered a 16 house quench during the end of a proton-antiproton colliding beam store followed by the damage of 2 collimators used for halo reduction at the CDF and DØ interaction points (Fig. 1). In addition, a cryogenic spool piece that houses correction elements was also damaged as a result of helium evaporation and pressure rise during the quench, requiring 10 days of Tevatron downtime for repairs.

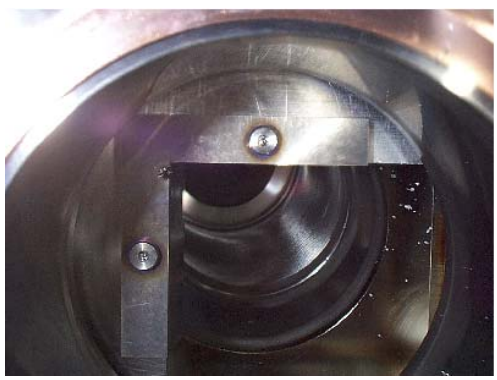

Figure 1: Damage to D49 5-mm thick tungsten primary collimator.

The initial reason of the large quench was found to be caused by a CDF Roman Pot reinserting itself back into the beam after it had been issued retract commands. The Roman Pot motion control hardware has since then been found to be faulty. This event prompted an investigation in order to describe the sequence of events to understand the damage imposed on the collimator devices.

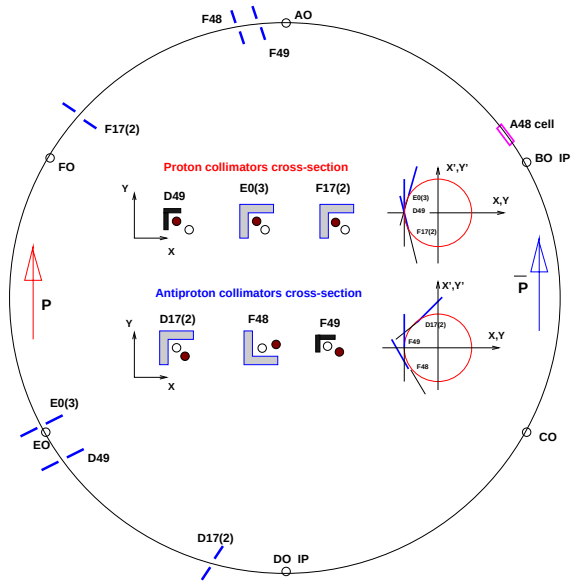

Figure 2: Tevatron Run II beam collimation system.

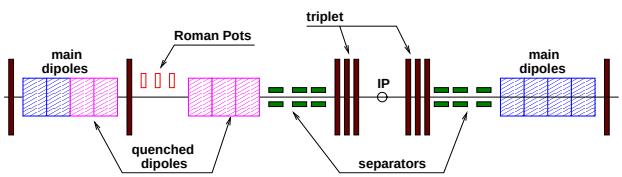

Figure 3: Schematics of the BØ interaction region with its Roman Pots and quenching cell A48.

BEAM DYNAMICS AT MAGNET CELL QUENCH

Fig. 2 shows the layout of the Tevatron and its Run II beam collimation system [1]. Normally, the beam scraping is done by the primary collimators at $5\sigma_{x,y}$ and secondary ones at $7\sigma_{x,y}$ at the beginning of accelerator cycle flat top after beams are brought to collisions. After the scraping is done, all collimators are retracted back from the beam by 1 mm, which is approximately equal to $2\sigma_{x,y}$. After collimators retracting the primary halo builds up to $7\sigma_{x,y}$ and secondary halo to $9\sigma_{x,y}$ during about 70 seconds.

The analysis of accident has shown that the Roman Pot moving fast towards the beam stopped at 5 mm from

* Work supported by the Universities Research Association, Inc., under contract DE-AC02-76CH03000 with the U. S. Department of Energy.
† drozhdin@fnal.gov

the beam pipe center. The Roman Pot vessel was at $\sim 6\sigma_x$ from the beam center, producing a tremendous spray of secondaries in the downstream magnets. This caused quench of the A48 superconducting magnet cell (Fig. 3). The magnet current degradation at the quench was equal to about 500 A/s effecting a degradation rate of magnetic field in five dipole magnets of $\Delta B/B_o = 2.39\times10^{-6}$ per turn. As was shown using the STRUCT code [2], the circulating beam moves towards the D49 collimator jaw with a rate of $\sim$0.005 mm per turn, and reaches the jaw surface by its 3σ-amplitude particles in approximately 300 turns after the quench start.

Particle hits at the collimators and a hits time distribution are shown in Fig. 4. The entire beam is lost during about 400 turns (8.4 msec) starting from the turn number 400, mostly on the D49 primary collimator and EØ3 and F17(2) secondary collimators.

The creation of a groove in the vertical jaw of the primary collimator (Fig. 1) was simulated by shifting out the jaw with a rate of 0.003 mm per turn starting from the turn number 550.

ENERGY DEPOSITION IN COLLIMATORS

Using the beam loss distributions calculated in the previous section, detailed energy deposition modeling was performed with the MARS14 Monte Carlo code [3] for the D49 tungsten primary collimators. Fig. 5 shows two-dimensional contours of energy deposition density in a 0.5-mm layer of the collimator vertical jaw. One sees that energy deposition is noticeably larger at the downstream end of a 5-mm plate, because of an intense cascade development for a 980-GeV proton beam over 1.5 radiation length thickness. One can expect that a semi-conical groove is drilled in the vertical jaw, that is confirmed in next Section. The hole diameter at the downstream end is about 2.5-3 mm.

Calculations performed for the 1.5-m long L-shaped secondary collimators E03 and F17(2) have shown (Fig. 6) that a 250-mm long and 3-mm wide slot is created in the stainless steel collimator vertical jaws.

ABLATION OF THE TUNGSTEN COLLIMATOR

The interaction of intense proton pulses with the collimator can result in rapid local heating and ablation of primary collimator tungsten or secondary collimator stainless steel from the surface.

Following a standard approach in surface physics [4, 5], we define the desorption rate, or the number of atoms leaving the unit surface of the solid tungsten in unit time, as

$$dN = N_0 \nu e^{-E_D/kT}, \qquad (1)$$

where N_0 is the number of atoms on the unit surface, $\nu = 10^{13}\,\mathrm{sec}^{-1}$, and E_D is the surface energy per tungsten atom which is equal to the heat of vaporization per atom, k is the Boltzmann constant, and T is the absolute temperature. The tungsten heat of vaporization is $Q_v = 824\,\mathrm{kJ/mol} = 1.3683\cdot10^{22}\,\mathrm{J/atom}$ and $N_0 = \sqrt{2}/a^2$, where a is the lattice constant; for tungsten $a = 3.16$ Å.

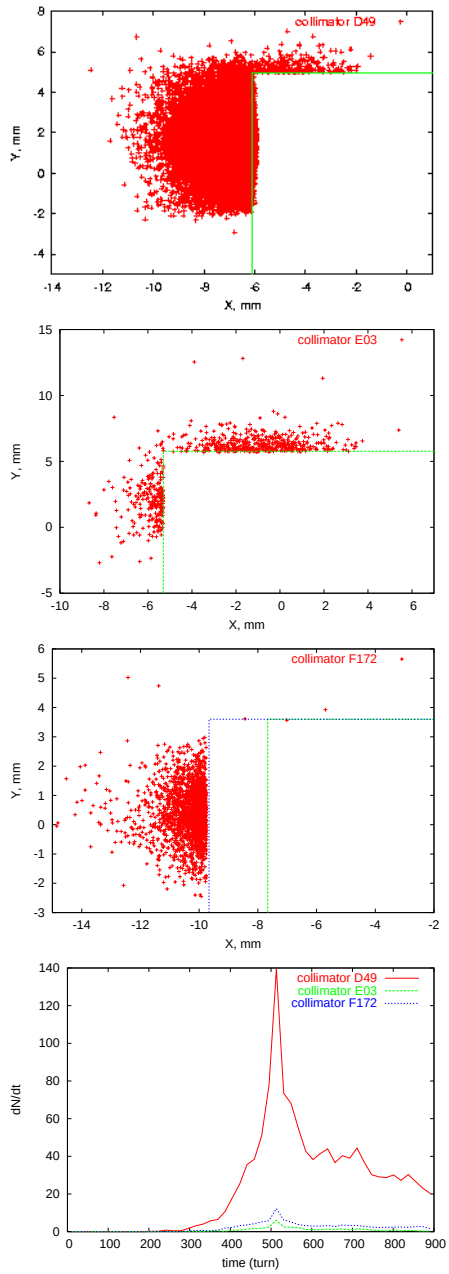

Figure 4: Particle hits at A48 cell quench in the collimators D49, E03 and F17(2), and hits time distribution.

The equation for the evolution of temperature in the collimator plate is

$$\frac{dT}{dt} = \frac{1}{C_p}\frac{dE_{\mathrm{ext}}}{dt} + \kappa\nabla T, \qquad (2)$$

where C_p is the specific heat at constant pressure, κ is the heat conductivity, and E_{ext} is the external energy deposited by the proton beam and calculated numerically using the MARS code.

Therefore, solving (2) and using (1), the normal displacement due to ablation of a surface element during time dt can be calculated as

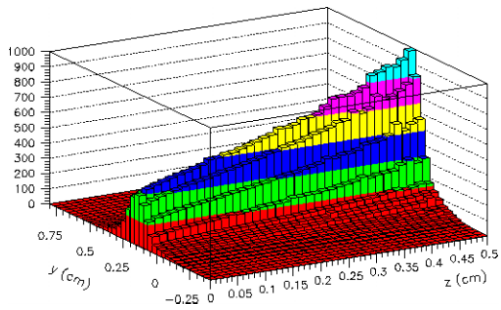

Figure 5: Energy deposition (J/g) isocontours in the D49 tungsten vertical jaw.

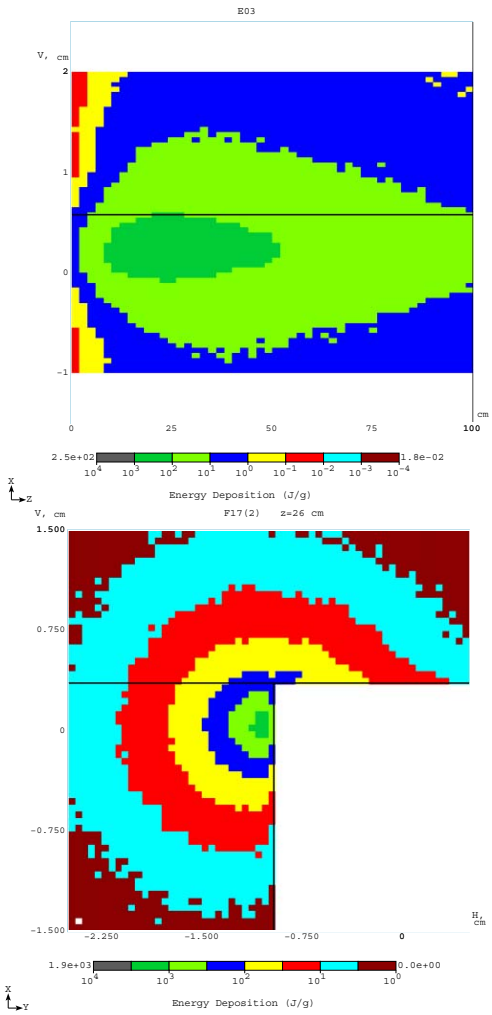

Figure 6: Energy deposition isocontours along the vertical jaw of E03 (top) and at shower maximum across the F17(2) (bottom) collimators.

$$dl = \frac{m_0 N_0 \nu dt}{\rho} e^{-Q_v/kT}, \qquad (3)$$

where the tungsten density $\rho = 19.35\,\mathrm{g/cm}^3$, and the atomic mass $m_0 = 183.85\,\mathrm{au} = 3.053 \cdot 10^{-22}\mathrm{g}$.

Numerical simulation results are given in Fig. 7. It shows the time evolution of the front and back surfaces of the collimator plate. We observe that the ablation of the back surface is much faster at early time due to cascade development in a 5 mm thick tungsten plate. At later time, the ablation rates at two surfaces are approximately equal.

Note that the numerical results presented here give the fast time limit estimate of the ablation process. This is due to the fact that some processes which may slightly slow down the ablation were neglected. These include the reduction of the internal energy of the collimator plate due to the kinetic and internal energy of the ablated material as the kinetic energy of the ablated material is unknown. The pressure of the ablated gaseous material was also neglected which may contribute during late stages of the ablation.

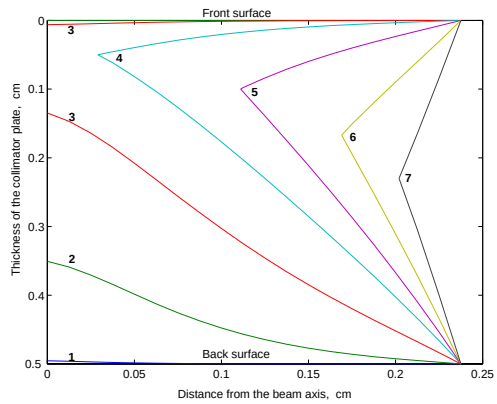

Figure 7: Evolution of the front and back surfaces of the collimator plate at $t = 0.4_{[1]} - 1.6_{[7]}\ ms$ with Δt=0.2 ms.

CONCLUSIONS

Analysis and simulations performed show that we have a good understanding of the entire picture of the December 2003 beam accident, both on dynamics and material damage sides. Calculated parameters of the hole and groove created in the collimators are very similar to those observed after the accident. There is work in progress to eliminate a possibility for such an accident in future. A new BLM system under consideration is to operate with multiple types of loss detection (average loss, fast and slow losses) and with independent abort threshold. The system will also have the capability to have different loss abort limits for different Tevatron states such as acceleration, injection and collisions.

REFERENCES

[1] M.Church, A.I.Drozhdin, A.Legan, N.V.Mokhov, R.Reilly, "Tevatron Run-II Beam Collimation System", Proc. 1999 PAC New York, p. 56, Fermilab-Conf-99/059 (1999).

[2] I.S.Baishev, A.I.Drozhdin, N.V.Mokhov, "STRUCT Program User's Reference Manual", SSCL–MAN–0034, 1994; http://www-ap.fnal.gov/∼drozhdin/

[3] N.V.Mokhov, "The MARS Code System User's Guide", Fermilab-FN-628,1995; "Status of MARS Code",Fermilab-Conf-03/053, 2003; http://www-ap.fnal.gov/MARS/.

[4] G. Iche, P. Nozieres, J. Phys. (Paris), **37** (1976), 1313.

[5] J. Davenport, G. Dienes, R. Johnson, Phys. Rev. B, **25** (1982), 2165-2174.